Journal of New Materials for Electrochemical Systems 17, 243-249 (2014)

New Strategy of Using Stannic Oxide as Catalyst in a Three-dimension Electrode Reactor for the Electro-oxidation of Organic Matter

Peng Li[1], Yuemin Zhao[2], Lizhang Wang[1,*], Binbin Ding and Yunlong Hu[3]

[1]School of Environment Science and Spatial Informatics, China University of Mining and Technology, Xuzhou City, Jiangsu 221008, PR China
[2]School of Chemical Engineering and Technology, China University of Mining and Technology, Xuzhou City, Jiangsu 221008, PR China
[3]Xuzhou Engineering Consulting Center, Xuzhou City, Jiangsu 221008, PR China

Received: June 10, 2014, Accepted: September 15, 2014, Available online: November 26, 2014

Abstract: *An efficient organic-matter (OM) degradation strategy using synthetic electrocatalysis particles as fixed filler in a three-dimension electrode reactor was developed. In our work, SnO_2-granular active carbon (SnO_2-GAC) was prepared by integrating GAC with nano-SnO_2 via the sol-gel method, using $SnCl_4$ as starting material and gelatin as a stabilizer. The phase composition and micro-morphology of the particles were characterized by X-ray diffraction, X-ray photoelectron spectroscopy and scanning/transmission electron microscopy techniques. The results showed the incorporation of SnO_2 crystallized in a tetragonal lattice with an average crystallite size of 10.6 nm, which was easily accessible on the GAC surface and mesopores. Electrochemical properties were tested with cyclic voltammetry and electrochemical impedance spectroscopy methods that disclosed an improved response current with a simultaneous increase in anodic area, while the charge-transfer and electrolyte resistance obviously decreased, in contrast to the virgin GAC filler in the three-dimension electrode system. Although the energy consumption of SnO_2-GAC (11.71 $kWh \cdot kg^{-1}$ COD) presented slight superiority than that of GAC (13.62 $kWh \cdot kg^{-1}$ COD) at the same chemical oxygen demand (COD) conversion of 98 % when a current density of 20 $A \cdot m^{-2}$ was employed for phenolic wastewater treatment, the required degradation time of the former (47.22 h) is greatly decreased compared with that of the latter (54.24 h). These results obviously confirm the superiority of the prepared SnO_2-GAC in electro-oxidation of organic matters.*

Keywords: Stannic oxide; three-dimension electrode reactor; organic matter; energy consumption

1. INTRODUCTION

Water that contains organic matter (OM) pollutant discharged from chemical syntheses, organic pesticides, and chlor-alkali production, as well as coking process, is universally recognized as recalcitrant and inimical towards traditional chemical and microbiological treatment technologies. For the purification of such wastewaters, advanced oxidation process (AOPs) by agents with exceptional oxidizing power, such as hydroxyl radicals (•OH), are considered particularly useful. Among the various AOPs, electrochemical degradation (ECD), which is environmental compatibility and suitable for low-volume application [1], has been a focus of attention for the industrial and academic research communities. In this process, reactive hydroxyl radicals could be generated by water discharge through the retardation of oxygen at high electrode overpotential [2-4], to detoxify macromolecular OMs or effect complete mineralization. Low cost electrodes with high stability and catalytic activity have been intensively studied for such purposes [5–6]. Electrodes prepared with SnO_2, besides the excellent properties mentioned above, are also distinguished for their high chlorine and oxygen evolution overpotential (2.20 V vs. reversible hydrogen electrode (RHE)) [7], and are thus satisfactory for organic pollutant elimination. Nevertheless, given the much higher resistivity of SnO_2 than other metal oxides (e.g., PbO_2 and RuO_2), its catalytic advantages have only been revealed after doping with Sb, Gd, Ru, and Ir species [8–10]. Furthermore, for SnO_2 electrodes,

*To whom correspondence should be addressed: Email: dhxktz@126.com
Phone: +86 516 83591320; Fax: +86 516 83591320

the restricted effective reaction area that participates in OM destruction remains an obstacle to achieving a satisfactory chemical oxygen demand (COD, mol $O_2 \cdot m^{-3}$) removal efficiency with reduced energy consumption (E_{sp}, kWh·kg^{-1} COD).

Electrochemical reactions require larger current and electrode area for charge gaining and lossing toward target reactants at solid-liquid interface; thus, materials possessing these functions synchronistically would be desirable. For a confined furtherance in the conductivity and the irregular shape of anode, fixed fillers can be tailored to give the highest electrocatalytic behavior and best pore properties. Based on this concept, researches [11-14] have been performed to fabricate and optimize packing materials. The possible approaches were focused on mechanical mixing and the impregnation of active semiconductor oxides in a substrate (usually granular activated carbon, GAC). With respect to homogeneity, uniformity, and conductivity, the latter method seemed to be a better approach to facilitate this incorporation. Ominde [12] reported that MnO_2-AC material displayed an excellent oxygen reduction capacity than activated carbon. Zhang [13] and Xu [14] found that efficient phenol degradation would be conducted with fabricated Mn-Sn-Sb/γ-Al_2O_3 and Mn-Sn-Sb/Ceramic particles, respectively. However, in the early reports, the systems suffered from metal oxide leakage, and a complete electrochemical characteristics analysis has not been performed with respect to OM degradation performance.

In this work, stannic oxide was used as an anodic component in a new strategy which does not improve electrical conductivity or involve lattice doping; rather, the SnO_2 was integrated into the GAC surface to produce a catalytic fixed filler. Nanostructuring is documented to be very helpful in intercalating nano-SnO_2 into GAC pores [12], which would impart a higher probability for an effective, increased interfacial area as well as prohibit GAC from plugging by OM degradation inside the GAC pore structures. So, it is reasonable to believe that productive OM elimination accompanied with reduced power depletion would be delivered. To comprehensively investigate the physical and electrochemical properties of this novel particle, various techniques including X-ray diffraction (XRD), X-ray photoelectron spectroscopy (XPS), scanning electron microscopy (SEM), transmission electron microscopy (TEM), cyclic voltammetry (CV), and electrochemical impedance spectroscopy (EIS) were conducted. All the results confirmed the excellent electrocatalytic ability of the SnO_2-GAC particles over the virgin GAC.

2. EXPERIMENTAL

2.1. Preparation of SnO_2-GAC

Spherical activated carbon made from bamboo, with an average particle size of ~5.0 mm and a specific surface area of 284 $m^2 \cdot g^{-1}$, was used as the substrate (Qing Lv Corp., Guangzhou, China). Before the preparation of the composite, the GAC was washed several times with distilled water and oven-dried for 2 d at 105°C to a constant weight. The SnO_2-GAC was prepared by the sol-gel method. Stannic tetrachloride solution (0.0261 kg $SnCl_4$ in 200 mL distilled water) was dissolved in gelatin (0.025 kg in 800 mL distilled water) at 60°C for obtaining of a clear gelatin solution [15]. Then, the GAC was introduced into the synthesized sol to form a raw coated layer. After aging for 2 to 3 d, the sample was dried in air at 105°C for 7 h and then baked at 500°C under nitrogen for 2.5 h.

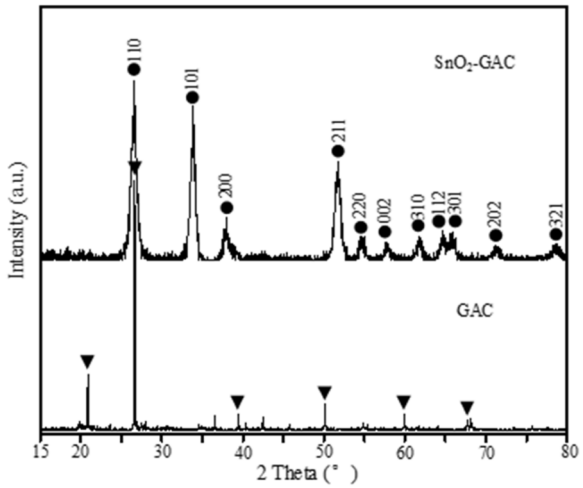

Figure 1. XRD patterns of GAC and SnO_2-GAC particles: ● SnO_2, ▼C.

2.2. Characterization Methods

The structure and phase composition of the SnO_2-GAC composite were investigated by powder XRD (D8 Advance, Cu Kα, Bruker, Germany) and XPS (ESCALAB 250Xi, Thermo Fisher, USA). The surface areas and porosities of the GAC and SnO_2-GAC particles were analyzed with an ASAP 2460 accelerated surface area and porosimetry system (Micrometrics, USA) by nitrogen adsorption at 77 K. Morphologies were observed by field-emission SEM (FESEM, Quanta 250, FEI, USA) and TEM (Tecnai G2F20, FEI, USA). CV and EIS, conducted with an IM6 electrochemical workstation (Zahner, Germany) in 0.25 mol·L^{-1} Na_2SO_4 and 0.01 mol·L^{-1} phenol solution, were carried out to study the catalytic properties of GAC and SnO_2-GAC toward phenol electrooxidation.

2.3. Bulk Electrolysis

Static experiments were performed using a poly (methyl methacrylate) reactor with dimensions of 10 cm × 10 cm × 5 cm (with electrodes spaced at 5 cm intervals) using a Ti/PbO_2 (Baoji Qixin Titanium Co., Ltd., China) anode and Ti cathode at a current density of 20 A·m^{-2}. For the electrical conductivity differences between GAC and SnO_2-GAC particles, cell voltages for the two packed systems were 2.76 and 2.43 V, respectively. Simulated wastewater containing 0.25 mol·L^{-1} Na_2SO_4 electrolyte and 0.01 mol·L^{-1} phenol was treated and COD values were determined by the COD_{Cr} method [16]. The results were used to calculate the COD conversion efficiency X based on equation (1):

$$X = \frac{COD_0 - COD_t}{COD_0} \quad (1)$$

where COD_0 and COD_t are the COD values initially and at time t (mol $O_2 \cdot m^{-3}$).

It is worth noting that at the beginning of bulk electrolysis experiments, GAC and SnO_2-GAC were soaked (10 h, 4 times) in raw water to reduce the impact on COD levels caused by physical absorption.

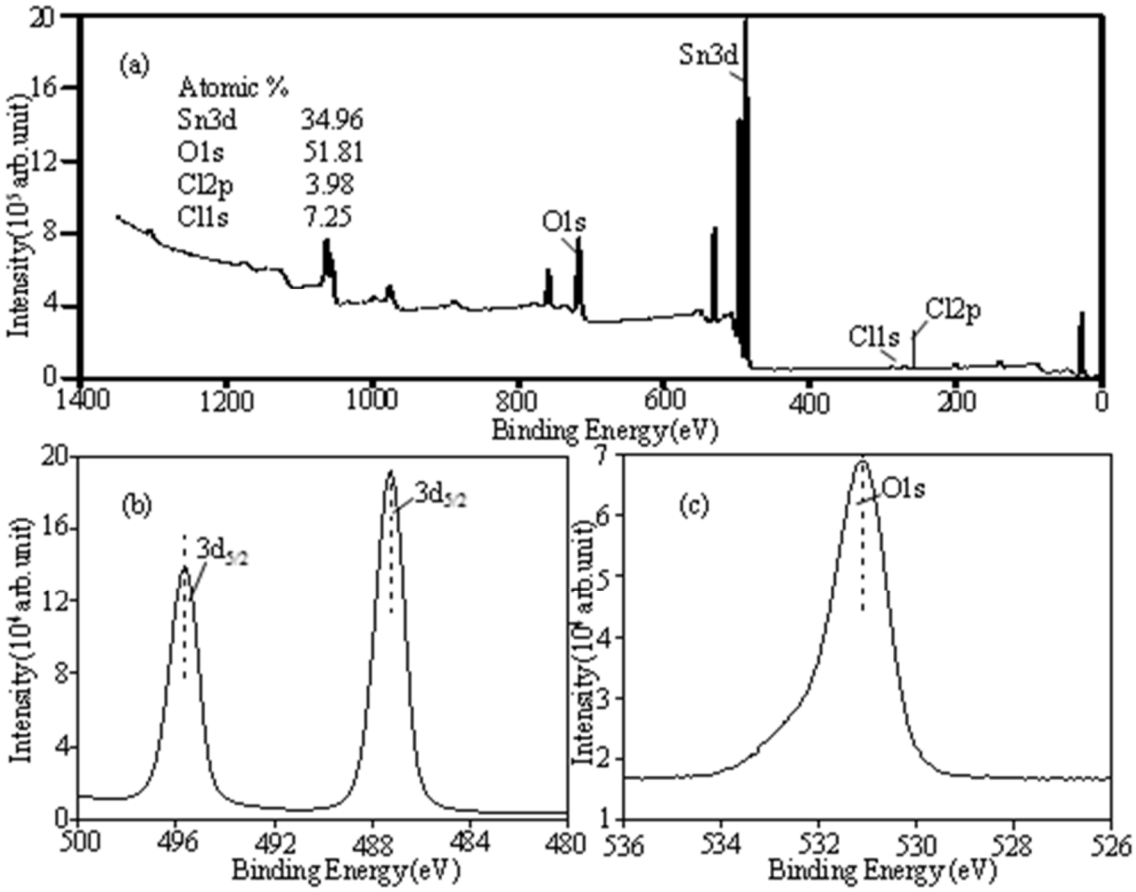

Figure 2. XPS survey spectrum (a), Sn3d spectrum (b), and O1s spectrum (c) of stannic oxide grains prepared by sol-gel method

2.4. Analysis Methods

The average crystallite size (D) of the SnO_2 on the GAC surface could be determined by the Scherrer equation [17]:

$$D = \frac{k\lambda}{\beta_{hkl}\cos\theta} \tag{2}$$

where λ is the wavelength of radiation (1.5406 Å for Cu Kα radiation), β_{hkl} is the half-width of the lattice plane (hkl), k is a constant equal to 0.94, and θ is the diffraction angle.

The energy consumption (E_{sp}, kWh·kg^{-1} COD) was calculated using eq. (3) [18], in which different equations are employed for the current-control and mass-transport-control stages during the galvanostatic OM degradation process.

$$E_{sp} = \frac{1}{3600}\frac{F}{8}\frac{V_c}{\eta} = \begin{cases} \dfrac{1}{3600}\dfrac{F}{8}V_c, & i < i_{lim} \\ \dfrac{1}{3600}\dfrac{F}{8}\dfrac{1-\alpha[1+\ln(\frac{1-X}{\alpha})]}{X}, & i > i_{lim} \end{cases} \tag{3}$$

where F is the Faraday constant (96487 C·mol^{-1}), 8 is the equivalent mass of oxygen, V_C is the cell voltage (V), $\overline{\eta}$ is the average current efficiency, and α is defined as i/i^0_{lim}.

Additionally, the critical time (t_{cr}) is defined to distinguish the two regimes, at which the applied current density (i) is equal to the limiting current density (i_{lim}) [19, 20]. Based on this, the duration of the current-control stage (t_{cr}) could be calculated through the formula for the limiting current density (eq. (4)), as displayed in eq. (5):

$$i_{lim(t)} = 4Fk_mCOD_t \tag{4}$$

$$t_{cr} = \frac{1-\alpha}{\alpha}\frac{V_R}{Ak_m} \tag{5}$$

Where A is the electrode area (m^2), k_m is the mass transport coefficient, V_R is the volume of the electrolyte (m^3).

The mass transport coefficient was proposed based on hydrodynamic conditions (Reynolds and Schmidt numbers) and the boundary effect factor (H_R/y_0) reported from our earlier study [21].

$$\kappa_m = \sqrt{\frac{iSc^{1/3}D}{nFc_o\varepsilon d_P(H_R/y_0)^{0.544}}(0.765\mathrm{Re}_P^{0.18}+0.345\mathrm{Re}_P^{0.614})} \tag{6}$$

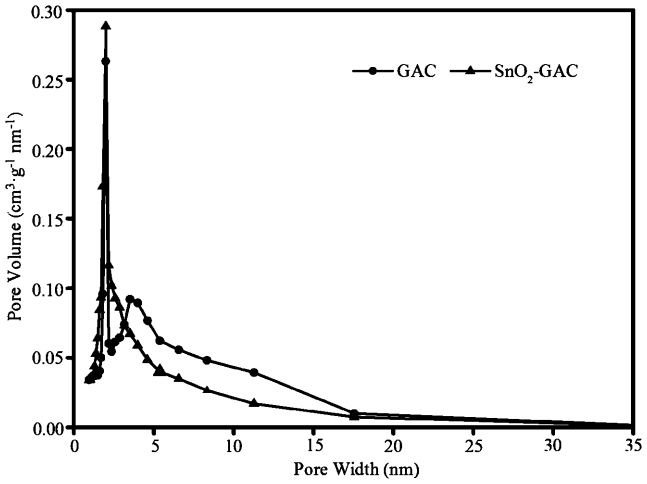

Figure 3. Pore distributions of GAC and SnO_2-GAC particles

where S_C is the Schmidt number, D is the diffusion coefficient, n is the charge transfer number, c_0 is the initial phenol concentration, ε is the bed porosity (0.51), d_p is average diameter for the transferred molecule, H_R is the hydraulic radius, y_0 is the height of the electrode, and Re_p is the Reynolds number.

3. RESULTS AND DISCUSSION

3.1. Sample Characterization

The XRD patterns of GAC and SnO_2-GAC prepared using the sol-gel method are presented in Fig. 1. Sharp, intense diffraction peaks that indicate the presence of carbon were observed on the GAC surfaces based on the PDF card (JCPDS Card No 65-6212). However, after intercalation treatment, the diffraction peaks for carbon decreased greatly. Evidence for the carbon substrate was only found at the diffraction angle 26.542°. The XRD pattern of the SnO_2-GAC particles confirmed the presence of stannic oxide grains on the GAC surface, with selected diffraction peaks at 2θ = 26.611°, 33.893°, 37.949°, and 42.634°, as supported by JCPDS Card No 41-1445. Furthermore, all the detected diffraction peaks can be indexed to the tetragonal lattice structure of single-phase SnO_2 [15, 22]. Relevant literature [23, 24] has discerned that stannic oxide in the tetragonal lattice structure demonstrates high electrocatalytic activity for OM oxidation. The average grain crystallite size of the stannic oxide, calculated with the Scherrer equation using the (110) peak, is 10.6 nm, indicating that nano-SnO_2 could permeate into the pore structures of the GAC [12], which is a prerequisite for pore electrocatalysis.

The XPS spectra of SnO_2-GAC are shown in Fig. 2. The survey spectrum and the data listed in Fig. 2 (a) illustrate that tin and oxygen atoms are predominantly distributed on the surface of the GAC, with an atomic ratio of 1:1.53, respectively. In the Sn3d spectrum, shown in Fig. 2(b), two peaks at 486.7 and 495.2 eV are found, indicative of Sn^{+4}. The high-accuracy O1s spectrum in Fig. 2 (c) reveals that oxygen is mostly bonded to tin, with a peak at a binding energy of 530.6 eV [20]. Previous studies have shown that, on SnO_2 surfaces, OMs undergo an electrochemical "combustion" process, i.e., total oxidation to CO_2 and H_2O, as depicted in eqs. (7)

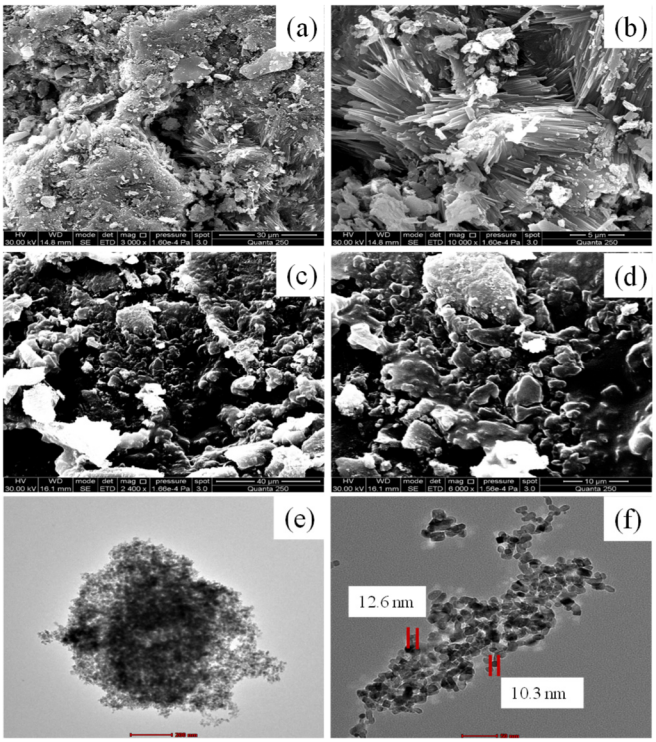

Figure 4. SEM images of GAC (a, b) and SnO_2-GAC (c, d), as well as TEM micrographs for SnO_2-GAC (e, f).

and (8) [25, 26]. In practice, the GAC surface and pores become deactivated by the adsorbed polymeric products as OM degradation proceeds in a three-dimension electrode reactor with GAC filler [27]. However, in the presence of stannic oxide, the resulting films can be removed and convenient channels for both liquid and solid OMs would be provided. Furthermore, because of the additional oxidation by the activated SnO_2 on the GAC surface, faster OM degradation with lower power consumption may be realized.

$$SnO_2 + H_2O \rightarrow SnO_2(OH\cdot) + H^+ + e^- \quad (7)$$

$$R + SnO_2(OH\cdot)n \rightarrow CO_2 + nH^+ + ne^- + SnO_2 \quad (8)$$

In terms of pore size distribution, an overwhelming majority of micropores (0–4 nm) and a lesser number of mesopores (4–15 nm) were observed on the pristine GAC surface (Fig. 3). After the introduction of the nano-SnO_2, the pore volume for the micropores increased slightly due to the sintering collapse of GAC internal structures or mesopore blocking by the stannic oxide grains. Nevertheless, the mesopore volume obviously decreased, although some large cracks may have been converted into mesopores after coating with SnO_2. Through the grain size calculation (10.6 nm for SnO_2 grains), we found that the entrance of micropores by SnO_2 is impossible, and active component of SnO_2-GAC particles spreading in mesoporous and its vicinal surface. Such phenomena could also be seen in the SEM images. The surface areas for GAC and SnO_2-GAC calculated by the Brunauer-Emmett-Teller (BET) method

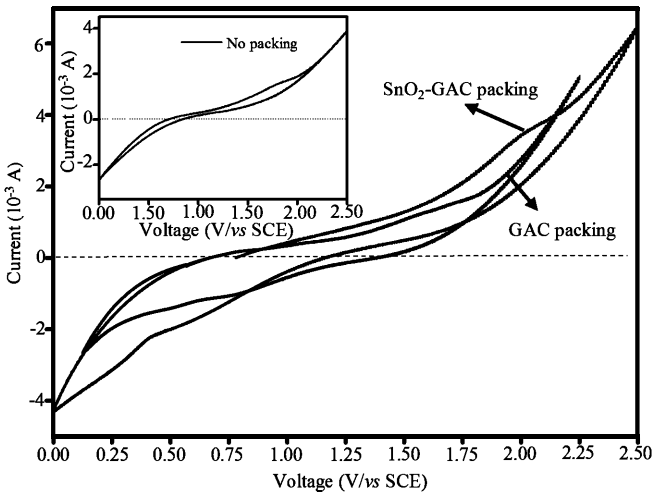

Figure 5. Cyclic voltammograms of GAC and SnO_2-GAC. Inset: cyclic voltammogram without filler. Scanning speed: 50 mv·s^{-1}

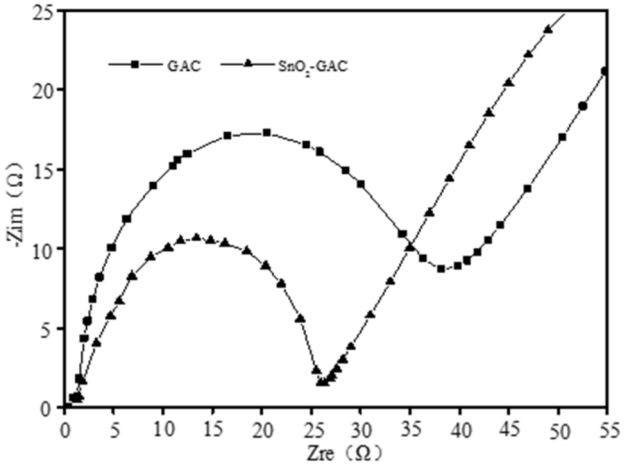

Figure 6. EIS spectra of GAC and SnO_2-GAC measured at open circuit potential in a three-dimension electrode reactor

were 284 and 312 m^2g^{-1}, respectively. The enlarged proportion of micropores by calcination and mesopore blocking would be responsible for this change.

The microstructures and surface morphologies were observed by SEM, and representative micrographs for GAC and SnO_2-GAC are shown in Fig. 4 (a, b) and (c, d), respectively. Cracks and pore structures occupy most of the GAC surface area, whereas a well-crystallized grain "membrane" with a relatively homogeneous grain distribution is observed with stannic oxide. Furthermore, the visible mesopores in the SEM images disappear, consistent with the decreased mesopore volume from Fig. 3. TEM is typically the principal method for characterizing the microstructure of nanocrystalline materials (particle size and shape) [23]. TEM micrographs for SnO_2-GAC are shown in Fig. 4 (e, f). The micrographs reveal that the SnO_2 grains are spherical or/and tetragonal in shape, and the average size of the particles (≈11.4 nm) is quite close to the calculated size based on X-ray crystallites. The uniform grain distribution also confirms the results obtained from SEM. The tetragonal structure and homogeneous well-organized distribution of stannic oxide underlie the material's outstanding electrochemical properties.

3.2. Electrochemical Properties

CV and EIS were employed to evaluate the electrochemical properties of SnO_2-GAC during OM oxidation using phenol as the degradation target with a conventional three-electrode system: a PbO_2/Ti anode, Ti cathode, and saturated calomel electrode (SCE) as reference. The container dimensions was 4×4× 3 cm, and the electrodes were spaced at 3 cm intervals.

Two irreversible CV curves without remarkable redox peaks are recorded in Fig. 5. Here, the "capacitance behavior" ignited by the faradic charge transfer on the GAC surface may be responsible for this unfamiliar phenomenon, and further investigations of this are in progress. It is obvious that the feedback current and the area under the CV curve for the three-dimension packed electrode reactor process were almost twofold compared to unpacked one; the increase may be attributed to the anode extension [28] by the bipolar GAC particles. Furthermore, compared with GAC packing, a larger feedback current and CV curve area were observed when SnO_2-GAC was used. This behavior may be related to changes in the chemical structure of SnO_2, such as hydration of the –Sn=O bond and formation of non-stoichiometric oxides (SnO_{2+x} or/and Sn_2O_{5+x}) for the further oxidation of phenol [29]. Through integration of the CV curves (positive direction along the *y*-axis), the voltammetric charges for phenol oxidation during CV scanning for the three conditions (no packing, packed with GAC, and packed with SnO_2-GAC) were 0.00749 C, 0.0114 C, and 0.0131 C, respectively. Since the true anode area, given by the geometric area, is 16 cm^2, then the anode areas for GAC and SnO_2-GAC as fixed fillers in the three-dimension electrode reactor can be calculated as 24.35 and 27.98 cm^2, respectively. Based on this, conclusion could be drawn that an enlarged feedback current was obtained because of the SnO_2 chemical structure and the improvement in the anode extension ability by GAC after the integration of stannic oxide.

EIS measurements carried out in the frequency range from 100 kHz to 10 mHz at the open circuit potential with an AC perturbation of 5 mV are showed in Fig. 6. Clearly, both impedance plots are similar, consisting of a semicircular component at high frequency followed by a linear component at low frequency. In the high frequency region, the intercept of the real impedance axis yields the electrolyte resistance (R_s), and the diameter of the semicircle denotes the charge transfer resistance (R_{ct}) [30]. As shown in Fig. 6, the R_s and R_{ct} values in the three-dimension electrode reactor with GAC and SnO_2-GAC fillers are 18.6 and 20.4 Ω, and 15.3 and 16.5 Ω, respectively. Obvious decreases in R_s and R_{ct} were obtained with stannic oxide impregnation. We suggest these two decreases result from the self-immunization of the electrode toward the polymeric derivative film, which occurs through the film destruction by active SnO_2 and the abundant channels available for charge transport after the nano-SnO_2 is incorporated into GAC pores. At low frequencies, two straight lines with slopes of approximately 60° were recorded. However, based on the steeper slope for SnO_2-GAC, we can conclude that SnO_2-GAC also holds great potential for electrochemical energy storage [31].

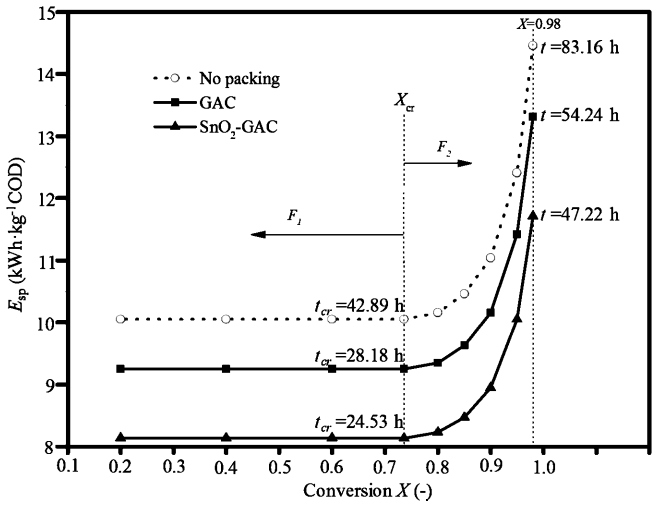

Figure 7. Energy consumption (E_{sp}) at different COD conversions (X) with SnO_2-GAC and GAC packing, and without packing in a three-dimension electrode reactor

3.2. Bulk Electrolysis

Bulk electrolysis experiments were conducted to purify phenolic wastewater and validate the improved OM degradation efficiency and lower power consumption of the fabricated electrocatalytic particles. Synthetic wastewater with a phenol concentration of 0.01 mol·L^{-1} in a 0.25 mol·L^{-1} sodium sulfate electrolyte were treated using GAC and SnO_2-GAC as the fixed fillers. The experiments were conducted under galvanostatic conditions with a current density of 20 A·m^{-2}. The results are shown in Fig. 7.

An obvious decrease in energy consumption was observed when a packed-type reactor was used for phenol electro-oxidation. As for the three-dimension electrode reactors packed with SnO_2-GAC and GAC particles, it is easier for the former to convert to the mass–transfer-controlled stage (F_2) from the current-controlled period (F_1), with an energy consumption of 8.14 kWh·kg^{-1} COD in 25 h. Based on equations (4) and (1), the boundary of these two stages occurs at X_{ct} = 0.736. For the GAC system, a higher E_{sp} (9.15 kWh·kg^{-1} COD) and longer reaction time (28 h) were required for the onset of F_2, compared to the faster phenol degradation rate (25 h for F_2) and lower energy consumption (8.14 kWh·kg^{-1} COD) when using the electrocatalytic SnO_2-GAC particles as the fixed filler. The acceleration in OM conversion speed and power savings could be significantly superior over long-term operation, to reach a relatively high COD removal rate of 98% for example, the electrochemical degradation process using SnO_2-GAC as the filler could be shortened by as much as 7.02 h while conserving 1.91 kWh·kg^{-1} COD compared with pristine GAC. Additionally, as listed in Table. 1, SnO_2-GAC as a fixed filler in the three dimensional electrochemical reactor performed in this work dispalys a much higher catalytic property for OMs electro-oxidation than many other methods reported in the previous literatures.

The bulk electrolysis experiments disclosed an uncontroversial OM degradation performance after the introduction of stannic oxide on the GAC surface. Because of its easy preparation and defined architecture, this electrocatalytic particle holds great promise for generalized applications in OM elimination in the three-dimension electrode reactor.

4. CONCLUSION

In this study, SnO_2-granular activated carbon particles were prepared via the sol-gel method using stannic tetrachloride as the starting material and gelatin as a stabilizer. Analytical techniques such as XRD, XPS, and SEM/TEM as well as surface area and pore distribution analyses were employed to physically characterize the material. The particles' electrocatalytic properties were evaluated by CV, EIS, and bulk electrolysis experiments using a simulated phenol containing wastewater. From these results, a new strategy for the use of stannic oxide was clearly revealed: stannic oxide can participate in the degradation of organic matter without being limited by its poor electrical conductivity and confined anodic area through its combination with granular activated carbon. Tetragonal SnO_2 with an average crystallite size of 10.6 nm was uniformly distributed on the GAC surface and mesopores. For this reason, decreased charge-transfer and electrolyte resistance was obtained in the three-dimension electrode reactor when SnO_2-GAC was used as the filler compared with GAC alone. The acceleration in OM conversion and power-saving performance of the novel particle composite was validated by phenol degradation. The reported work has confirmed the superior electrochemical oxidation performance of SnO_2-GAC over virgin GAC.

Table. 1. Comparation of the reported SnO_2-GAC as fixed filler in the three dimension electrode reactor with other electrochemical methods

Item / Method	Electrodes	Packing	Wastewater	COD or c conversion rate/ %	E_{sp}/ kWh·kg^{-1} COD
Reference[32]	Stainless steel	GAC	Phenol	73	16.39
Reference[33]	Graphite	B-GAC	Aniline	76-78	-
Reference[34]	RuO_2/Ti	Pd-GAC	Haloacetic acids	90-95	-
Reference[35]	BDD	-	Phenol	100	13.50
This work	PbO_2/Ti	GAC	Phenol	98	13.62
This work	PbO_2/Ti	SnO_2-GAC	Phenol	98	11.71

c is the concentration of the mentioned wastewater, mg·L^{-1}.

5. ACKNOWLEDGEMENTS

This work was supported by a grant from the program of the Natural Science Foundation of China for Innovative Research Groups (No.51221462), the National Natural Science Foundation of China (No.50908226), the Jiangsu Provincial Research Foundation for Graduate Education in Innovation and Engineering (CXLX13-956) and the innovation and venture fund for college students of China University of Mining and Technology.

REFERENCES

[1] F.C. Walsh, Pure Appl. Chem., 73, 1819 (2001).
[2] Y.J. Feng, X.Y. Li, Water Res., 37, 2399 (2003).
[3] A.M. Polcaro, S. Palmas, F. Renoldi, M. Mascia, Electrochim. Acta, 46, 389 (2000).
[4] G. Siné, C. Comninellis, Electrochim. Acta, 50, 2249 (2005).
[5] C.C. Jara, G.R. Salazar-Banda, R.S. Arratia, J.S. Campina, Chem. Eng. J., 171, 1253 (2011).
[6] X. Yang, R. Zou, F. Huo, D. Cai, D. Xiao, J. Haz. Mat., 164, 367 (2009).
[7] F. Vicent, E. Morallòn, C. Quijada, J. Appl. Electrochem., 28, 607 (1998).
[8] H. Bi, C. Yu, W. Gao, P. Cao, Electrochim. Acta, 113, 446 (2013).
[9] Y. Feng, Y. Cui, B. Logan, Z. Liu, Chemosphere, 70, 1629 (2008).
[10]X. Chen, G. Chen, P.L. Yue, J. Phys. Chem. B, 105, 4623 (2001).
[11]L. Wang, Y. Zhao, J. Fu, J. Haz. Mat., 160, 608 (2008).
[12]N. Ominde, N. Bartlett, X.-Qing. Yang, D. Qu, J. Power Sources, 185, 747 (2008).
[13]Z. Fang, L.G. Ming, S. Yi, H. Huikang, W. Hua, Acta Chem. Sin., 64, 235 (2006).
[14]X. Haiqing, L.X. Ning, W.Y. Qiao, W.H. Lin, S.Y. Ming, Acta Phys. Chim. Sin., 25, 840 (2009).
[15]A. Khorsand Zak, A. Moradi Golsheikh, W. Haliza Abd Majid, S.M. Banihashemian, Mater. Lett., 109, 309 (2013).
[16] "Standard methods for examination of water and wastewater, 20th ed." APHA, Washington, DC, 1998.
[17]K. Fukuda, K. Kikuya, K. Isono, M. Yoshio, J. Power Sources, 69, 165 (1997).
[18]M. Panizza, P.A. Michaud, G. Cerisola, C. Comninellis, Electrochem. Commun., 3, 336 (2001).
[19]M. Panizza, P.A. Michaud, G. Cerisola, C. Comninellis, J. Electroanal. Chem., 507, 206 (2001).
[20]M.A Rodrigo, P.A. Michaud, I. Duo, M. Panizza, G. Cerisola, C. Comninellis, J. Electrochem. Soc., 148, D60 (2001).
[21]L. Wang, Y. Hu, Y. Zhang, P. Li, Y. Zhao, Sep. Purificat. Technol., 109, 18 (2013).
[22]Q. Li, X. Yuan, G. Zeng, S. Xi, Mater. Chem. Phys., 47,239 (1997).
[23]D. Guo, Z. Jing, J. Colloid Interface Sci., 359, 257 (2011).
[24]L. Zhang, L. Xu, J. He, J. Zhang, Electrochim. Acta, 117, 192 (2014).
[23]Y.M. Abbas, S.A. Mansour, M.H. Ibrahim, S.E. Ali, J. Magnetism Magnetic Mater., 324, 2781 (2012).
[25]R.A. Torres, W. Torres, P. Peringer, C. Pulgarin, Chemosphere, 50, 97 (2003).
[26]C.C. Jara, G.R. Salazar-Banda, R.S. Arratia, J.S. Campino, M. I. Aguilera, Chem. Eng. J., 171, 1253 (2011).
[27]V.V. Panić, A.B. Dekanski, T.R. Vidaković, V.B. Mišković, B.Ž. Javanović, B.Ž. Nikolić, J. Solid State Electrochem., 9, 43 (2005).
[28]L. Wang, P. Li, Q. Yan, Water Sci. Technol., 66, 422 (2012).
[29]C. Comninellis, C. Pulgrarin, J. Appl. Electrochem., 23, 108 (1993).
[30]S. Yang, H.H. Song, X. Chen, Electrochem. Commun., 8, 137 (2006).
[31]Y. Liu, D. Yan, Y. Li, Z. Wu, R. Zhuo, S. Li, J. Feng, J. Wang, P. Yan, Z. Geng, Electrochim. Acta, 117, 528 (2014).
[32]Y. Xiong, C. He, H.T. Karlsson, X.H. Zhu, Chemosphere, 50, 131 (2003).
[33]S. Kaerhikeyan, K. Viswanathan, R. Boopathy, P. Maharaja, G. Sekaran. J. Ind. Eng. Chem., Inpress (2014).
[34]X. Zhao, A.Z. Li, R. Mao, H.J. Liu, J.H. Qu, Water Res., 51, 134 (2014).
[35]M. Panizza, A. Kapalka, C. Comninellis, Electrochim. Acta, 53, 2289 (2008).